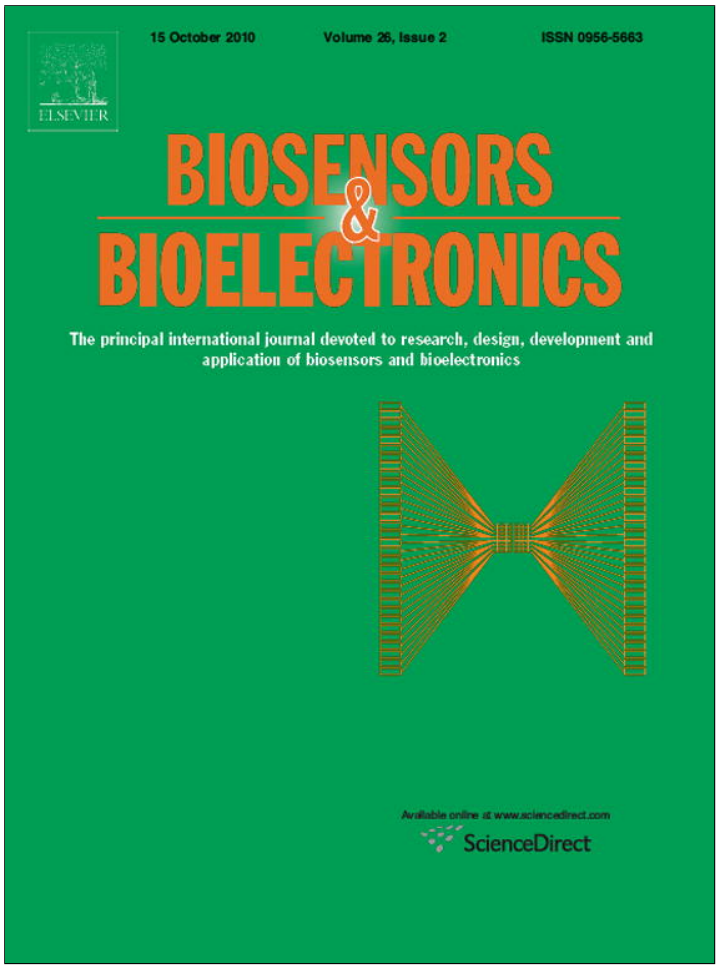

Biosensors and Bioelectronics 26 (2010) 432–436

Contents lists available at ScienceDirect

Biosensors and Bioelectronics

journal homepage: www.elsevier.com/locate/bios

Pt-dispersed flower-like carbon nanosheet aggregation for low-overpotential electrochemical biosensing

Sheng Tang[a], Xizhang Wang[b], Jianping Lei[a,*], Zheng Hu[b], Shengyuan Deng[a], Huangxian Ju[a,*]

[a] Key Laboratory of Analytical Chemistry for Life Science (Ministry of Education of China), Department of Chemistry, Nanjing University, Nanjing 210093, PR China
[b] Key Laboratory of Mesoscopic Chemistry (Ministry of Education of China), Department of Chemistry, Nanjing University, Nanjing 210093, PR China

ARTICLE INFO

Article history:
Received 20 April 2010
Received in revised form 24 July 2010
Accepted 26 July 2010
Available online 1 August 2010

Keywords:
Biosensor
Electrochemistry
Pt nanoparticles
Glucose oxidase
Flower-like carbon nanosheet aggregation

ABSTRACT

A Pt nanoparticle-decorated flower-like carbon nanosheet aggregation (FCNA) was prepared via one-step ethylene glycol method. The aggregation was characterized with scanning electron micrographs, X-ray photoelectron spectra, X-ray diffraction and electrochemical impedance spectra. When the aggregation was immobilized on a glassy carbon electrode, the dense dispersion of Pt nanoparticles (Pt NPs) on the carbon nanosheets of FCNA could combine the good conductivity of FCNA with the excellent catalytic activity of Pt NPs for the electroreduction of oxygen at a low overpotential, which led to a method for electrochemical detection of oxygen from 6.3 to 69.3 μM. Using glucose oxidase (GOx) as a model, the resulting GOx/Pt/FCNA nanocomposite-based amperometric biosensor showed a linear response to glucose ranging from 0.5 to 8.0 mM with a detection limit of 0.3 mM at a S/N ratio of 3. The designed biosensor was of excellent performance with high selectivity, acceptable recovery and good repeatability, and could be successfully applied in the detection of glucose in human serum. The FCNA could be expected as a carrier for the preparation of other metal nanoparticle-dispersed aggregations and biosensing applications.

1. Introduction

Recent trends in development of biosensors have increasingly emphasized on the application of various nanomaterials to improve their analytical performance (Deng et al., 2008; Fu et al., 2009; Sarma et al., 2009; Tsai et al., 2009; Tyagi et al., 2009). Especially, carbon materials have attracted considerable interest in electrochemical applications due to their unique properties, such as high electrical conductivity, relatively wide potential window, and low background current (Kim et al., 2007; Wu et al., 2009). However, because the relatively less defect sites on the pristine carbon materials lead to low-efficient catalysis and high overpotential, the further functionalization of carbon materials with metal nanoparticles has been expected to be excellent candidate for biosensor design.

Platinum nanoparticles (Pt NPs) have been extensively employed as functional materials for preparation of fuel cells due to their high catalytic activity toward methanol oxidation (Mu et al., 2005; Kongkanand et al., 2006; Zhang et al., 2007a; Seidel et al., 2010). The catalytic ability of Pt NPs is strongly related to their size, size distribution, and the carrier. A facile route to fabricate the nanohybrids of Pt–carbon nanotubes (CNTs) has been developed for the glucose sensing by a template method (Wen et al., 2009). Although CNTs have been thought to be an attractive carrier material for noble metal nanoparticles due to the unique mechanical and electronic properties (Chen et al., 2009; Dumitrescu et al., 2009; Park et al., 2009), preparing well-dispersed Pt NPs on CNTs is still a challenge due to their winding surface. So a material with large surface-to-volume ratio and planar surface is desirable as a support for efficiently immobilizing Pt NPs for glucose biosensing.

The detection of glucose in blood is one of the most frequent performances for human health (Newman and Turner, 2005; Heller and Feldman, 2008). Although the third-generation biosensors, based on the direct electron transfer between the cofactor FAD of glucose oxidase (GOx) and the electrode, show good promising in glucose detection due to the decrease of interference (Jing and Yang, 2006; Liu et al., 2007; Wu et al., 2007b; Zhang et al., 2007b; Wang, 2008; Deng et al., 2009; Yang et al., 2009; Zeng et al., 2009; Li et al., 2010; Santafe et al., 2010), the direct electron transfer for oxidation of $FADH_2$ or reduction of FAD is hard to realize at conventional electrodes because the FAD is deeply embedded within the protein shells (Shan et al., 2009; Wang et al., 2009). Thus, developing novel Pt NPs-functionalized carbon nanomaterials will provide good candidates for convenient preparation of glucose biosensor with a low detection potential.

* Corresponding authors. Tel.: +86 25 83593593; fax: +86 25 83593593.
E-mail addresses: jpl@nju.edu.cn (J. Lei), hxju@nju.edu.cn (H. Ju).

0956-5663/$ – see front matter © 2010 Elsevier B.V. All rights reserved.
doi:10.1016/j.bios.2010.07.105

Flower-like microconstruction is composed of a number of 1- or 2-dimensional subunits with one end aggregating together. The microconstruction can give a relatively high specific surface area, evenly distributed mesoporosity and chemical stability, which are favorable for its application as electrode materials (Xiao et al., 2006; Shen and Feng, 2008). Moreover, the graphite flakes of flower-like petals could provide a significant support for efficiently immobilizing nanoparticles (Wu et al., 2004). Here, a flower-like carbon nanosheet aggregation (FCNA) with a number of 2-dimensional planar subunits was introduced as a support for preparation of well-dispersed Pt NPs via one-step ethylene glycol method. Based on the excellent electrocatalytic activity of the Pt NPs and the good conductivity of FCNA, the reduction of oxygen was realized at −0.05 V. The overpotential for oxygen reduction was lower than −0.16 V at nitrogen-doped carbon nanotubes modified electrode (Deng et al., 2009), exhibiting good promise in inhibiting the interference of coexisted species. Using GOx as a model, a biosensor was developed for electrochemical detection of glucose based on the consumption of O_2 upon addition of glucose. The biosensor could be successfully applied in the detection of glucose in human serum. The FCNA provides a useful platform for constructing the enzyme-based biosensors.

2. Materials and methods

2.1. Reagents

FCNA was prepared by means of removable template. Briefly, a certain amount of nano-size magnesium oxide as template was first heated in argon flow of 50 standard cubic centimeter per minute. Benzene vapor was then introduced to this system for 1 h to deposited carbon on the template. Finally, the template was removed by 1.0 mol L^{-1} HCl solution. Hexachloroplatinic acid ($H_2PtCl_6{\cdot}6H_2O$) was purchased from Shanghai Reagent Co. Glucose oxidase (GOx, EC 1.1.3.4, type X-S, lyophilized power, 100–250 units mg^{-1}, from Aspergillus niger) was purchased from Sigma. D-(+)-Glucose was bought from Sinopharm Chemical Reagent Co., Ltd. Glucose stock solution was mutarotated overnight at room temperature prior to use. Multi-walled carbon nanotubes (MWCNTs) with diameter of 40–60 nm were obtained from Shenzhen Nanotech Port Company. All other chemicals were of analytical grade. High purity nitrogen was used for deaeration. O_2 solutions with different concentrations were prepared by injecting different volumes of O_2-saturated water into 0.1 M pH 7.0 phosphate buffer solution (PBS).

2.2. Apparatus and electrochemical measurements

Scanning electron microscopic (SEM) images were obtained using a Hitachi S-4800 scanning electron microscope (Hitachi, Japan). X-ray diffraction (XRD) was measured on Philips X'pert Pro X-ray diffractometer with Cu Ka radiation of 1.542 Å. X-ray photoelectron spectra (XPS) were obtained on a K-Alpha X-ray photoelectron spectrometer (Thermo Fisher Scientific Co., USA). The concentration of blood sugar in human serum was measured with Hitachi 7180 automatic biochemical analyzer (Hitachi, Japan). Electrochemical impedance measurements were carried out on a PGSTAT30/FRA2 system (Autolab, The Netherlands) in 0.1 M KCl solution containing 5.0 mM $K_3[Fe(CN)_6]/K_4[Fe(CN)_6]$. Cyclic voltammetric experiments were performed with conventional three-electrode system consisting of a glassy carbon electrode (GCE) as working, a saturated calomel electrode as reference and a platinum wire as counter electrodes on a CHI 812B electrochemical workstation (CH Instruments Inc., USA). The electrochemical responses of the biosensor for glucose were detected with cyclic voltammetry in air-saturated 0.1 M pH 7.0 PBS at 0.1 V s^{-1}.

2.3. Preparation of Pt/FCNA composite and biosensors

Pt/FCNA composite was prepared according to the ethylene glycol method (Li et al., 2003; Yue et al., 2008), which has been a routine method to disperse Pt nanoparticles on the sidewall of MWCNTs (Yue et al., 2008). 10.0 mg FCNA was suspended in 10.0 mL ethylene glycol and sonicated for 20 min to obtain a liquid suspension. 0.4 mL of H_2PtCl_6 solution (15.8 mg mL^{-1}) was added to the suspension dropwise and magnetically stirred for 3 h. After adjusting the pH of the suspension to above 11.0, the overall mixture was refluxed at 140 °C for 3 h to ensure the sufficient reduction of the Pt species by ethylene glycol. The solid sample denoted as Pt/FCNA was collected after thorough rinsing with ethanol several times and drying at 110 °C for 12 h. The resulting solid sample was about 23% Pt loading on FCNA. For comparison, Pt/MWCNTs catalyst was prepared with the same procedure by replacing FCNA with MWCNTs (diameter 40–60 nm), whose circumference is comparable to the width of planar subunits of FCNA (about 100–200 nm). The obtained solids were redispersed in water with a concentration of 1.0 mg mL^{-1}.

The GCE was successively polished to a mirror finish using 1.0 and 0.05 μm alumina slurry (Beuhler) followed by rinsing thoroughly with double-distilled water. After successive sonication in ethanol and double-distilled water, the electrode was rinsed with double-distilled water and allowed to dry at room temperature.

When doping with different volumes of Pt/FCNA (1.0 mg mL^{-1}) on the GCE, the corresponding current increased with the increasing volume from 3.5 to 8.5 μL, and reached a platform after 7.5 μL. Thus, 7.5 μL of Pt/FCNA (1.0 mg mL^{-1}) suspension as the optimal volume was dropped on GCE surface and dried at room temperature to form Pt/FCNA modified GCE. The Pt/FCNA modified GCE was then immersed into 0.1 M PBS containing 2.0 mg mL^{-1} GOx for 20 h at 4 °C in refrigerator. The resulting GOx/Pt/FCNA modified GCE was rinsed throughout with double-distilled water to wash away the loosely adsorbed enzyme molecules. For comparison, GOx/Pt/MWCNTs and GOx/FCNA modified GCEs were prepared with the same procedure. All enzyme-modified electrodes were stored in 0.1 M pH 7.0 PBS at 4 °C in refrigerator when not in use.

3. Results and discussion

3.1. Characterization of Pt/FCNA

The SEM image of Pt/FCNA displayed a flower-like microstructure with the diameter of around 5 μm (Fig. 1A). Several flower-like microstructures could be observed from the SEM image with wide area (Fig. S1A). The microstructure was composed of many curled and overlapped nanosheets with the thickness less 10 nm, which should provide a significant increase of effective area for enzyme loading. Compared with FCNA structure (Fig. 1B), the well-dispersed Pt NPs were observed on the carbon nanosheets (Fig. 1C) with the size range from 3 to 9 nm. The small size of Pt NPs could lead to highly efficient catalytic activity to oxygen reduction. After the immobilization of GOx, a mushy GOx/Pt/FCNA film was observed (Fig. S1B), proving the efficient capturing of GOx on the surface of Pt/FCNA.

Fig. 1D shows the XRD patterns of the Pt/FCNA composite. The small diffraction peak at 30° is attributed to (0 0 2) plane of graphitized FCNA. The peaks at 39.7°, 46.4°, 67.7° are assigned to the (1 1 1), (2 0 0), (2 2 0) planes of Pt NPs, respectively, indicating face-centered cubic structure (Li et al., 2009; Zhang et al., 2010). Therefore, the XRD results suggested that Pt species were reduced

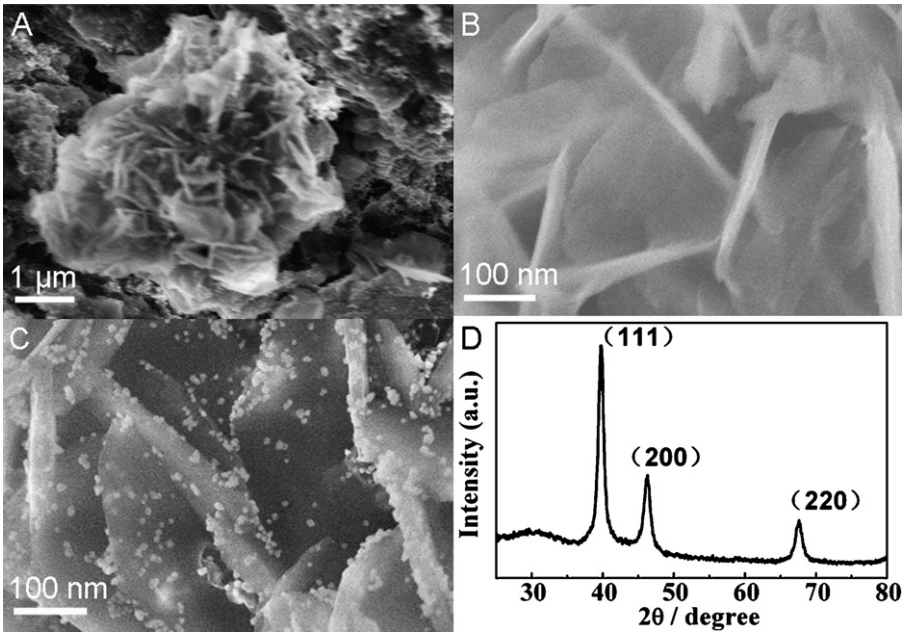

Fig. 1. (A) SEM image of Pt/FCNA, amplified SEM images of (B) FCNA and (C) Pt/FCNA, and (D) XRD of Pt/FCNA.

to the metallic state with good crystalline on FCNA via the ethylene glycol method.

XPS was employed to further analyze the chemical composition and status of the Pt/FCNA. As shown in Fig. S2A, the XPS survey scan spectrum of Pt/FCNA exhibited distinct O 1s, C 1s and Pt 4f peaks, while FCNA exhibited only O 1s and C 1s peaks, indicating that FCNA were quite stable as catalyst support and remained its composition and status after Pt loading. The O 1s peak might originate from PtO_x species or the unavoidable adsorbed oxygen on the sample. The Pt 4f peaks located at 71.9 and 74.5 eV (Fig. S2B), corresponding to Pt $4f_{7/2}$ and $4f_{5/2}$ respectively. The peak area of oxidized Pt species (Pt(II) and Pt(IV)) was about 27% of total peak area (Fig. S2B), indicating the predominant composition of the loaded Pt NPs was Pt(0) species. The small amount of oxidized Pt species (Pt(II) and Pt(IV)) might be responsible for the incomplete reduction of the Pt species (Villers et al., 2006).

Using $[Fe(CN)_6]^{3-/4-}$ redox couple as the electrochemical probe, the Nyquist plots of different electrodes in the frequency range from 0.01 to 100,000 Hz were shown in Fig. 2. The electron transfer resistance, R_{ct}, could be calculated according to the equivalent circuit (inset in Fig. 2). At a bare GCE the redox process of the probe showed an electron transfer resistance of about 350 Ω (curve a), which was larger than that of FCNA modified GCE (curve b), indicating that FCNA could act as a good electron-transfer interface between the probe and electrode. After assembling 23% Pt NPs, the electron transfer resistance further decreased to 150 Ω (curve c). Moreover, the electron transfer resistance slightly decreased with the increasing deposition of Pt NPs (curves d and e). The decrease of electron transfer resistance confirmed the presence of Pt NPs on FCNA, and indicated that the Pt/FCNA microcomposite could be used as an efficient platform for construction of electrochemical devices.

3.2. Electrocatalysis toward O_2 reduction at Pt/FCNA modified GCE

In order to investigate the effect of Pt NPs loading, 13%, 23% and 37% Pt loading on FCNA were prepared. The response to O_2 increased with the increasing Pt NPs loading from 13% to 23% (Fig. S3) and then trended to slight increase. So, 23% Pt NPs loading was chosen in this work. Fig. 3 shows the cyclic voltammogram of Pt/FCNA (23% Pt) modified electrode in 0.1 M PBS solution with different concentrations of O_2. In the potential window from +0.4 to −0.3 V, the Pt/FCNA exhibits good electrocatalysis toward the reduction of O_2. The starting potential of O_2 reduction occurs at +0.3 V, which is much more positive than those of −0.2 V at multi-wall CNTs (Dai and Shiu, 2004) and −0.05 V at mesoporous carbon-tetrathiafulvalene composite modified electrodes (Ndamanisha et al., 2010). The peak potential of oxygen reduction is −0.05 V, at which the peak current shows a linear calibration range from 6.3 to 69.3 μM with the sensitivity of 4.1 mA cm^{-2} mM^{-1}. The sensitivity is also much higher than 0.723 mA cm^{-2} mM^{-1} of carbon nanofiber modified electrode (Wu et al., 2007a). Thus the modified electrode had good performance with low reduction potential and high sensitivity for determination of oxygen due to the highly efficient catalysis of Pt/FCNA composite.

Repeated use of the electrodes did not affect the long-term stability. The coefficients of variation of the current signals for six

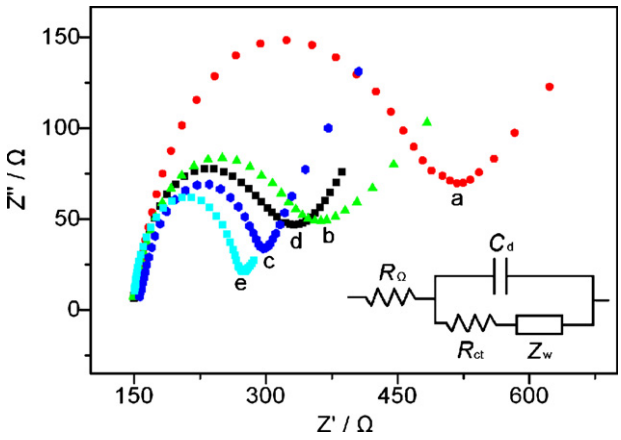

Fig. 2. Electrochemical impedance spectra of (a) bare, (b) FCNA, (c) 23% Pt/FCNA, (d) 13% Pt/FCNA and (e) 37% Pt/FCNA modified GCEs in 0.1 M KCl solution containing 5.0 mM $K_3[Fe(CN)_6]/K_4[Fe(CN)_6]$. Inset: equivalent circuit applied to fit impedance measurements in presence of $K_4[Fe(CN)_6]/K_3[Fe(CN)_6]$. $R_Ω$, the resistance of electrolyte solution; C_d, double-layer capacitance; Z_w, Warburg impedance; R_{ct}, electron transfer resistance.

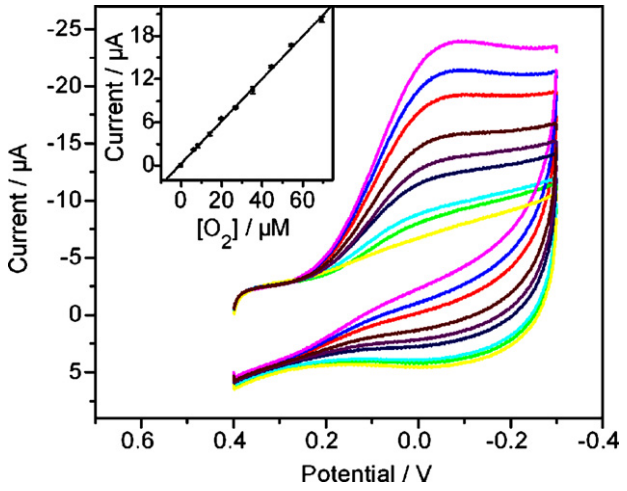

Fig. 3. Cyclic voltammograms of Pt/FCNA modified GCE in 0.1 M PBS (pH 7.0) containing 6.3, 8.3, 14.2, 19.9, 27.0, 35.3, 44.6, 54.4 and 69.3 μM oxygen from inner to outside. Inset: calibration curve corresponding to amperometric responses at −0.05 V. Scan rate: 0.1 V s^{-1}.

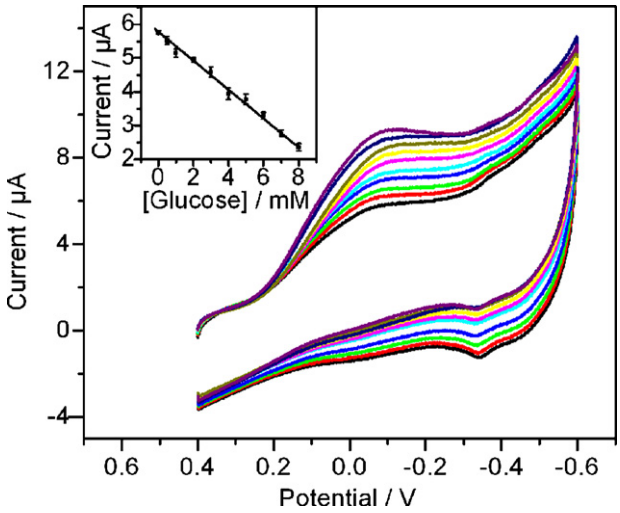

Fig. 5. Cyclic voltammograms of GOx/Pt/FCNA modified GCE in air-saturated PBS spiked with 0.5–8.0 mM glucose from outside to inner. Inset: calibration curve corresponding to amperometric responses at −0.08 V. Scan rate: 0.1 V s^{-1}.

repeated injections of 10.0 and 50.0 μM O_2 were 3.1% and 2.4%, respectively. The modified electrode showed acceptable preparation reproducibility with a relative standard deviation of 3.2% estimated from the slopes of the calibration plots at five freshly prepared Pt/FCNA modified electrodes. Thus, the resulting sensors exhibited good reproducibility for both the detection and preparation.

3.3. Biosensing application of GOx/Pt/FCNA modified GCE

The glucose biosensors are generally based on the detection of the oxidation signal of hydrogen peroxide at +600 mV or the reduction signal of dissolved oxygen at −600 mV, which is produced or consumed in the oxidation process of β-D-glucose to D-δ-lactone catalyzed by GOx, respectively. Based on the greatly enhanced reduction activity of dissolved oxygen at Pt/FCNA composite, a glucose biosensor was constructed by immobilizing GOx at the Pt/FCNA modified electrode. At this electrode glucose was selectively oxidized by oxygen in GOx enzymatic cycle, which decreased the oxygen concentration. The glucose concentration could thus be monitored by oxygen reduction signal.

As shown in Fig. 4, no obvious peak was observed in air-saturated PBS at the GOx/FCNA modified electrode. The

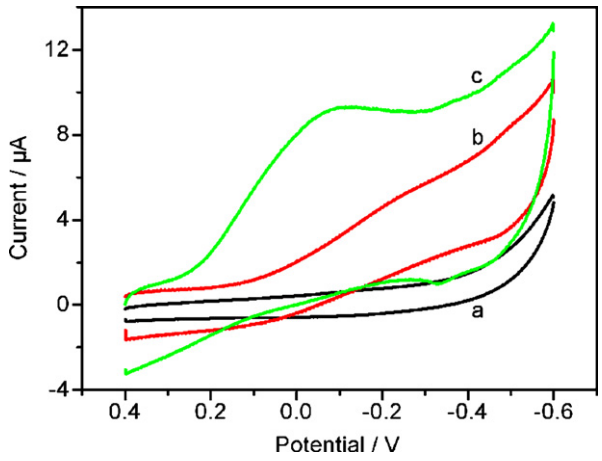

Fig. 4. Cyclic voltammograms of GOx/FCNA (a), GOx/Pt/MWNTs (b), and GOx/Pt/FCNA (c) modified GCEs in air-saturated 0.1 M PBS (pH 7.0). Scan rate: 0.1 V s^{-1}.

GOx/Pt/FCNA exhibited the electrocatalysis toward the reduction of O_2 with a reduction peak of −0.08 V, while the peak occurred at about −0.27 V at GOx/Pt/MWCNTs modified GCE. This result could be attributed to the presence of FCNA as support for better dispersion of Pt NPs than that in the presence of MWCNTs due to the abundant 2-dimensional planar subunits of the FCNA. The excellent catalytic activity of Pt/FCNA toward the reduction of dissolved oxygen and good selectivity of GOx resulted in highly selective and sensitive amperometric response to glucose at a low overpotential of oxygen reduction. It should be pointed out that when the peak potential of oxygen reduction shifted from −0.05 V at Pt/FCNA modified electrode to −0.08 V at GOx/Pt/FCNA modified electrode, the peak current decreased due to the presence of enzyme film.

Upon addition of glucose aliquot to air-saturated pH 7.0 PBS, the response of GOx/Pt/FCNA modified GCE to oxygen reduction decreased linearly in the glucose concentration range from 0.5 to 8.0 mM with a detection limit of 0.3 mM at a S/N ratio of 3. The sensitivity was 6.0 μA mM^{-1} cm^{-2} (Fig. 5), which was higher than 1.06 μA mM^{-1} cm^{-2} at single-walled carbon nanohorns based biosensor (Liu et al., 2008) and 4.8 μA mM^{-1} cm^{-2} at laponite nanoparticles based biosensor (Shan et al., 2010). Since the blood–glucose level is normally maintained between 4.0 and 6.0 mM (Shan et al., 2009), the linear response range from 0.5 to 8.0 mM was suitable for the practical application of GOx/Pt/FCNA modified GCE in blood sugar monitoring.

The low reduction potential was an advantage for excluding the interference of other coexisted species. The effect of possible interfering species on glucose detection was examined using 3.0 mM uric acid or ascorbic acid, which caused an increase of 2.4% or 3.1% in the reduction current of 1.0 mM glucose, respectively (Fig. S4). This result suggested that the proposed glucose biosensor had high selectivity, and no interference from those endogenously coexisted electroactive substances due to the low operating potential.

The analysis of glucose was carried out in human serum without any need of sample pretreatment except a standard addition step by adding glucose into the sample. The recovery test was performed by adding 2.0 M glucose to two serum samples, which produced the recovery of 98.6% and 103.7%, demonstrating good accuracy for the determination of glucose in real samples. The concentrations of glucose in two serum samples were determined to be consistent with those obtained by spectrophotometric measurements (Table 1).

The performance of the glucose biosensor was further examined by successively detecting 4.0 mM glucose for 10 times, the relative

Table 1
Glucose concentrations in serum samples tested by the proposed method ($n = 3$) and spectrophotometric measurements.

Serum sample	Spectrophotometric measurements concentration (mM)	Proposed method concentration (mM)
Sample 1	5.49	5.65 ± 0.05
Sample 2	5.34	5.12 ± 0.04

standard deviation (RSD) was 6.0%, demonstrating a good repeatability. After 50 successive scanning the response was still retained 95.7% of the initial response, suggesting the acceptable durability of the biosensor. After each glucose detection, the current response of the proposed film modified GCE in blank PBS deceased by about 0.4%. In addition, the RSD of current signals for measurement of 4.0 mM glucose at five independently prepared biosensors was 3.4%, which proved good reproducibility of the biosensor preparation.

The stability of GOx/Pt/FCNA modified GCE and the corresponding background current was investigated when stored in 0.1 M pH 7.0 PBS at 4 °C and measured at intervals over several days (Fig. S5). After 10 days the response was still retained 97% value of the initial response, and after 20 days the response was still retained 94% value of the initial response. This implied that the GOx/Pt/FCNA modified GCE was high efficient for retaining the bioactivity of enzyme and preventing its leakage from the membrane.

4. Conclusions

A novel Pt NPs/FCNA composite was prepared via the one-step ethylene glycol method for low-overpotential reduction of oxygen. Due to the flower-like structure of FCNA, Pt NPs could be conveniently and densely dispersed on the carbon nanosheets without need of pre-surface modification. FCNA could accelerate the electron transfer, and Pt NPs could be employed as efficient catalyst. The resulting Pt/FCNA composite exhibited high electrocatalytic activity toward the reduction of O_2. To demonstrate the practical application of the electrocatalytic activity, a biosensor was constructed for the detection of glucose at low overpotential and successfully applied in the detection of glucose in real samples. The flower-like structure might provide a significant carrier for loading of metal nanoparticles and design of electrochemical biosensors.

Acknowledgements

This research was supported by National Natural Science Foundation of China (20821063, 90713015, 20705012, 20875044), National Basic Research Program of China (No. 2010CB732400) and PhD Fund of MOE for Young Teachers (20070284052).

Appendix A. Supplementary data

Supplementary data associated with this article can be found, in the online version, at doi:10.1016/j.bios.2010.07.105.

References

Chen, X.X., Eckhard, K., Zhou, M., Bron, M., Schuhmann, W., 2009. Anal. Chem. 81, 7597–7603.
Dai, Y.Q., Shiu, K.K., 2004. Electroanalysis 16, 1697–1703.
Deng, C.Y., Chen, J.H., Chen, X.L., Xiao, C.H., Nie, L.H., Yao, S.Z., 2008. Biosens. Bioelectron. 23, 1272–1277.
Deng, S.Y., Jian, G.Q., Lei, J.P., Hu, Z., Ju, H.X., 2009. Biosens. Bioelectron. 25, 373–377.
Dumitrescu, I., Unwin, P.R., Macpherson, J.V., 2009. Chem. Commun., 6886–6901.
Fu, C.L., Yang, W.S., Chen, X., Evans, D.G., 2009. Electrochem. Commun. 11, 997–1000.
Heller, A., Feldman, B., 2008. Chem. Rev. 108, 2482–2505.
Jing, W., Yang, Q., 2006. Anal. Bioanal. Chem. 385, 1330–1335.
Kim, S.N., Rusling, J.F., Papadimitrakopoulos, F., 2007. Adv. Mater. 19, 3214–3228.
Kongkanand, A., Kuwabata, S., Girishkumar, G., Kamat, P., 2006. Langmuir 22, 2392–2396.
Li, W.Z., Liang, C.H., Zhou, W.J., Qiu, J.S., Zhou, Z.H., Sun, G.Q., Xin, Q., 2003. J. Phys. Chem. B 107, 6292–6299.
Li, Y.M., Tang, L.H., Li, J.H., 2009. Electrochem. Commun. 11, 846–849.
Li, K.T., Liu, B., Zheng, J.B., Sheng, Q.L., Liu, R.X., 2010. Electroanalysis 22, 701–706.
Liu, G.Z., Paddon-Row, M.N., Gooding, J.J., 2007. Electrochem. Commun. 9, 2218–2223.
Liu, X., Shi, L., Niu, W., Li, H., Xu, G., 2008. Biosens. Bioelectron. 23, 1887–1890.
Mu, Y.Y., Liang, H.P., Hu, J.S., Wan, L.J., 2005. J. Phys. Chem. B 109, 22212–22216.
Ndamanisha, J.C., Bo, X.J., Guo, L.P., 2010. Analyst 135, 621–629.
Newman, J.D., Turner, A.P.F., 2005. Biosens. Bioelectron. 20, 2435–2453.
Park, H.S., Choi, B.G., Yang, S.H., Shin, W.H., Kang, J.K., Jung, D., Hong, W.H., 2009. Small 5, 1754–1760.
Santafe, A.A.M., Doumeche, B., Blum, L.J., Girard-Egrot, A.P., Marquette, C.A., 2010. Anal. Chem. 82, 2401–2404.
Sarma, A.K., Vatsyayan, P., Goswami, P., Minteer, S.D., 2009. Biosens. Bioelectron. 24, 2313–2322.
Seidel, Y.E., Schneider, A., Jusys, Z., Wickman, B., Kasemo, B., Behm, R.J., 2010. Langmuir 26, 3569–3578.
Shan, C.S., Yang, H.F., Song, J.F., Han, D.X., Ivaska, A., Niu, L., 2009. Anal. Chem. 81, 2378–2382.
Shan, D., Zhang, J., Xue, H.G., Ding, S.N., Cosnier, S., 2010. Biosens. Bioelectron. 25, 1427–1433.
Shen, J.M., Feng, Y.T., 2008. J. Phys. Chem. C 112, 13114–13120.
Tsai, T.W., Heckert, G., Neves, L.F., Tan, Y.Q., Kao, D., Harrison, R.G., Resasco, D.E., Schmidtke, D.W., 2009. Anal. Chem. 81, 7917–7925.
Tyagi, P., Postetter, D., Saragnese, D.L., Randall, C.L., Mirski, M.A., Gracias, D.H., 2009. Anal. Chem. 81, 9979–9984.
Villers, D., Sun, S.H., Serventi, A.M., Doletet, J.P., Desilets, S., 2006. J. Phys. Chem. B 110, 25916–25925.
Wang, J., 2008. Chem. Rev. 108, 814–825.
Wang, Z.Y., Liu, S.N., Wu, P., Cai, C.X., 2009. Anal. Chem. 81, 1638–1645.
Wen, Z.H., Ci, S.Q., Li, J.H., 2009. J. Phys. Chem. C 113, 13482–13487.
Wu, L.N., Zhang, X.J., Ju, H.X., 2007a. Biosens. Bioelectron. 23, 479–484.
Wu, S., Ju, H.X., Liu, Y., 2007b. Adv. Funct. Mater. 17, 585–592.
Wu, Y.H., Yang, B.J., Zong, B.Y., Sun, H., Shen, Z.X., Feng, Y.P., 2004. J. Mater. Chem. 14, 467–477.
Wu, Z., Zhen, Z., Jiang, J.H., Shen, G.L., Yu, R.Q., 2009. J. Am. Chem. Soc. 131, 12325–12332.
Xiao, Y., Liu, Y.L., Cheng, L.Q., Yuan, D.S., Zhang, J.X., Gu, Y.L., Sun, G.G., 2006. Carbon 44, 1589–1591.
Yang, L.Q., Ren, X.L., Tang, F.Q., Zhang, L., 2009. Biosens. Bioelectron. 25, 889–895.
Yue, B., Ma, Y.W., Tao, H.S., Yu, L.S., Jian, G.Q., Wang, X.Z., Wang, X.S., Lu, Y.N., Hu, Z., 2008. J. Mater. Chem. 18, 1747–1750.
Zhang, J., Sasaki, K., Sutter, E., Adzic, R.R., 2007a. Science 315, 220–222.
Zhang, J.D., Feng, M.L., Tachikawa, H., 2007b. Biosens. Bioelectron. 22, 3036–3041.
Zhang, S., Shao, Y.Y., Yin, G.P., Lin, Y.H., 2010. J. Mater. Chem. 20, 2826–2830.
Zeng, X.D., Li, X.F., Liu, X.Y., Liu, H., Luo, S.L., Kong, B., Yang, S.L., Wei, W.Z., 2009. Biosens. Bioelectron. 25, 896–900.